Structural, magnetic, and electronic transport properties of hole-doped $SrFe_{2-x}Cu_xAs_2$ single crystals

Y. J. Yan, P. Cheng, J. J. Ying, X. G. Luo, F. Chen, H. Y. Zou, A. F. Wang, G. J. Ye, Z. J. Xiang, J. Q. Ma, and X. H. Chen*

Hefei National Laboratory for Physical Science at Microscale and Department of Physics, University of Science and Technology of China, Hefei, Anhui 230026, People's Republic of China

(Received 2 December 2012; revised manuscript received 29 January 2013; published 6 February 2013)

We report the structural, magnetic, and electronic transport properties of $SrFe_{2-x}Cu_xAs_2$ single crystals grown by a self-flux technique. Both $SrCu_2As_2$ and $SrFe_2As_2$ crystallize in a $ThCr_2Si_2$-type (122-type) structure at room temperature, but exhibit distinct magnetic and electronic transport properties. According to the x-ray photoelectron spectroscopy Cu $2p$ core line position, resistivity, susceptibility, and positive Hall coefficient, $SrCu_2As_2$ is an *sp*-band metal with Cu in the $3d^{10}$ electronic configuration corresponding to the valence state Cu^{1+}. Compared with $SrCu_2As_2$, the almost unchanged Cu $2p$ core line position in $SrFe_{2-x}Cu_xAs_2$ indicates that partial Cu substitutions for Fe in $SrFe_2As_2$ may result in hole doping rather than the expected electron doping. No superconductivity is induced by Cu substitution on Fe sites, even though the structural/spin density wave transition is gradually suppressed with increasing Cu doping.

DOI: 10.1103/PhysRevB.87.075105 PACS number(s): 74.70.Xa, 74.25.F−, 74.62.Dh

I. INTRODUCTION

The exploration of new high-temperature superconductors and research on their superconducting mechanisms have always been the highlight in condensed matter physics. Especially, the discovery of a second class of high-temperature superconductors, iron-based superconductors, has reignited interest in high-temperature superconductivity research. There are five types of iron-based superconductors: 1111 with a ZrCuSiAs-type structure, 122 with a $ThCr_2Si_2$-type structure, 111 with a Fe_2As-type structure, 11 with an anti-PbO-type structure, and a newly discovered $K_xFe_{2-y}Se_2$ with a Fe vacancy which is called the 122* structure. Among these materials, compounds with a 122 structure have gained much attention because of the high superconducting temperature and ease in obtaining large high quality single crystals.

In the 122-type compound $BaFe_2As_2$, superconductivity can be induced by applying pressure,[1–3] and by substitutions at the Ba site (by K),[4] at the Fe site (by Co, Ni, Ru, Rh, and Pd),[5,6] and at the As site (by P).[7] It has been revealed that partial Co, Ni, Rh, and Pd substitutions at the Fe site in $BaFe_2As_2$ could induce superconductivity[8–11] with T_c up to 25 K, whereas no superconductivity is induced by Mn (Refs. 12–14) or Cr (Refs. 15 and 16) substitutions. As we know, the formal valence states of the atoms in $BaFe_2As_2$ are assigned as Ba^{2+}, Fe^{2+}, and As^{3-}, so the Fe atoms are formally in the $3d^6$ electronic configuration. These results suggest that the superconductivity might relate to the average number of $3d$ conducting electrons of the transition metal atom.[17] It means that electron doping at the Fe site by Co, Ni with more $3d$ electrons induces superconductivity, while hole doping by Cr, Mn with less $3d$ electrons does not. From this point of view, divalent copper Cu^{2+} with three more *d* electrons than Fe^{2+} should be a strong electron dopant for iron arsenide superconductors. However, even though the Cu substitution successfully suppresses the structural/spin density wave (SDW) transition of the parent compound,[18] superconductivity was not observed in the Cu-doped $BaFe_2As_2$. It is a very strange phenomenon that Cu substitution in iron-based superconductors shows a completely different character from that of Co and Ni substitutions. Electronic structure calculations for $SrCu_2As_2$ and $BaCu_2As_2$ by Singh[19] predicted that these compounds might be *sp*-band metals, where the Cu atoms have a formal valence state of Cu^{1+} and a nonmagnetic and chemically inert $3d^{10}$ electronic configuration. Anand *et al.* confirmed this result by measuring the electronic and magnetic properties of $SrCu_2As_2$ and $BaCu_2As_2$, suggesting that Cu substitution for Fe in $(Ca,Sr,Ba)(Fe_{1-x}Cu_x)_2As_2$ should result in hole doping.[17] Therefore, we speculate that the distinct valence state of Cu ions may be responsible for the unique behavior compared with other transition-metal-doped conditions.

To obtain insights into the nature of the puzzling properties of Cu-doped iron-based materials, we have synthesized a series of $SrFe_{2-x}Cu_xAs_2$ single crystals and investigated the valence state of copper ions by x-ray photoelectron spectroscopy (XPS) measurements, and their structural, magnetic, and electronic transport properties.

II. MATERIALS AND METHODS

A series of $SrFe_{2-x}Cu_xAs_2$ single crystals, from $SrFe_2As_2$ ($x = 0$) to $SrCu_2As_2$ ($x = 2.0$), were grown by a self-flux technique using high purity Sr, Cu, Fe, and As. Prereacted CuAs and FeAs were used as the flux. To synthesize $SrFe_{2-x}Cu_xAs_2$, Sr, FeAs, and CuAs fluxes with a molar ratio of $1{:}2.5(2-x){:}2.5x$ were placed into alumina crucibles and then sealed inside evacuated quartz tubes. The crystal growth was carried out by heating the samples to 1150 °C, holding them there for 24 h, and then cooling to 850 °C at a rate of 2 °C/h. The size of the obtained single crystals for $0 \leqslant x < 1.0$ and $1.0 \leqslant x \leqslant 2.0$ were typically $5 \times 3 \times 0.15$ mm^3 and $2.5 \times 2 \times 0.15$ mm^3, respectively.

The samples were characterized by x-ray diffraction (XRD) using a Rigaku D/max-A x-ray diffractometer with Cu $K\alpha$ radiation in the range of 10°–70° with steps of 0.01° at room temperature. The actual Cu and Fe concentrations of the single crystals were determined from energy-dispersive x-ray (EDX) analysis. The Cu content x hereafter is the actual composition determined by EDX. The valence state of Cu is determined

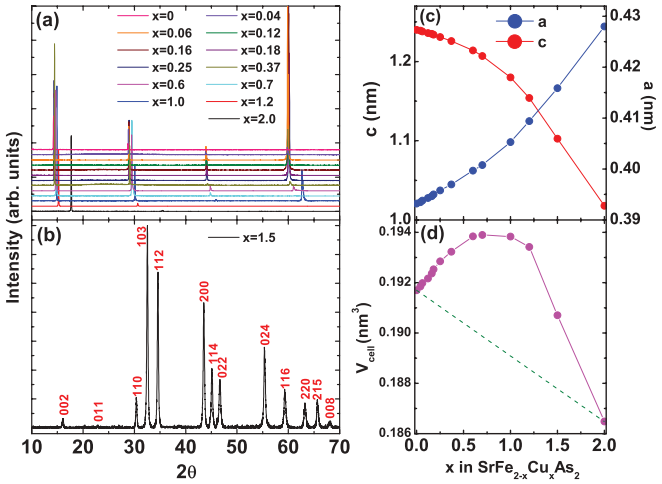

FIG. 1. (Color online) (a) Single crystal x-ray diffraction patterns for $SrFe_{2-x}Cu_xAs_2$ single crystals recorded at room temperature (x is the actual composition covering from 0 to 2.0). Only (00l) diffraction peaks are observed, indicating that the c axis is perpendicular to the plane of the single crystal. (b) Powder x-ray diffraction pattern for a $SrFe_{0.5}Cu_{1.5}As_2$ polycrystal recorded at room temperature. (c) Lattice parameters of the a and c axes as a function of x. The lattice parameters of the a and c axes were obtained by combining single crystal XRD and powder XRD patterns. The data for $x = 1.5$ are collected from the polycrystal. (d) The unit cell volume V as a function of x for $SrFe_{2-x}Cu_xAs_2$ single crystals. The green dashed line represents Vegard's law for this series of compounds.

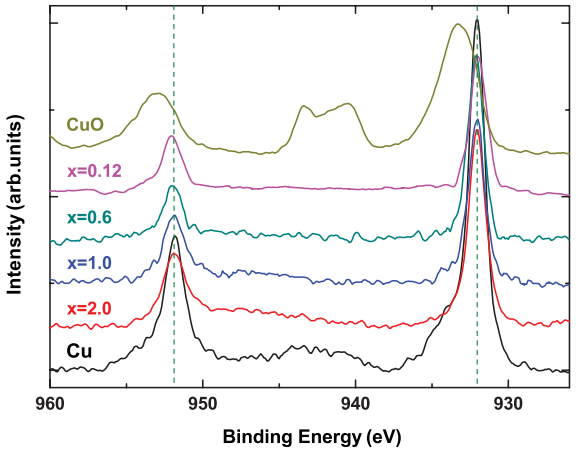

FIG. 2. (Color online) XPS Cu $2p$ spectra of Cu metal (where Cu is nominally in a Cu^{0+} state), CuO (where Cu is in a Cu^{2+} state), and $SrFe_{2-x}Cu_xAs_2$ single crystals with $x = 0.12$, 0.6, 1.0, 2.0 after background subtraction. The two dashed lines correspond to the binding energies of Cu $2p_{1/2}$ and Cu $2p_{3/2}$ in Cu metal.

by x-ray photoelectron spectroscopy (XPS). The resistivity was measured using the standard four-probe method by the Quantum Design Physical Property Measurement System (PPMS). Hall resistivity data were collected using the ac transport option of a Quantum Design PPMS in a four-wire geometry with switching the polarity of the magnetic field $H \parallel c$ to remove any magnetoresistive components due to the misalignment of the voltage contacts. Magnetic susceptibility was measured using a vibrating sample magnetometer (VSM).

III. RESULTS AND DISCUSSION

Figure 1(a) shows the single crystal XRD patterns for all the $SrFe_{2-x}Cu_xAs_2$ single crystals. Only (00l) diffraction peaks are observed, indicating that the single crystals are in perfect (001) orientation. The powder XRD pattern of the $SrFe_{0.5}Cu_{1.5}As_2$ polycrystal is shown in Fig. 1(b). All diffraction peaks can be indexed by a tetragonal structure with $a = 0.4158$ nm and $c = 1.1018$ nm, indicating that the sample is single phase. Figure 1(c) shows the evolution of the lattice parameters of the a and c axes as a function of Cu doping content. The lattice parameter of the c axis is obtained from the (00l) diffraction peaks, while that of the a axis is obtained by powder XRD. With increasing Cu doping content, the lattice parameter of the a axis increases monotonically, while that of the c axis decreases monotonically. The unit cell volume $V = a^2c$ first increases with increasing Cu content, reaches a maximum at about $x \sim 1.0$, and then decreases with further increasing Cu content. Obviously, the evolution of V for $SrFe_{2-x}Cu_xAs_2$ deviates from Vegard's law, which shows a linear decrease with Cu content. Ni *et al.*[18] reported the lattice parameters a and c and the unit cell volume V of $Ba(Fe_{1-x}Cu_x)_2As_2$ versus x up to $x = 0.35$, which shows a similar evolution of V to $SrFe_{2-x}Cu_xAs_2$. Singh[19] gave a theoretical prediction that Cu in $BaCu_2As_2$ and $SrCu_2As_2$ has a fully occupied stable d^{10} shell at high binding energy, which means that the valence state of Cu in these compounds is +1, while in $SrFe_2As_2$, the valence state of Fe is +2. Therefore, we conclude that the anomalous behavior of V of $SrFe_{2-x}Cu_xAs_2$ may indicate interesting changes of the valence state in the Cu/Fe sites. In order to confirm it, XPS measurements were performed on several samples. As shown in Fig. 2, the Cu2$p_{1/2}$ and Cu2$p_{3/2}$ binding energy maxima for Cu metal are about 951.9 and 932.0 eV, and the linewidths are very narrow. The lines in $SrFe_{2-x}Cu_xAs_2$ single crystals are a little broader than that in Cu metal, and their peak positions are nearly the same as those in Cu metal, which resemble those of Cu_2O, as reported previously,[20] while for CuO, the peak positions for divalent copper shift to higher binding energies, which are distinctly different than those of Cu^{0+} and Cu^{1+}. Furthermore, the linewidth in CuO is broader with a factor of 2, and the satellite is very intense. Considering these distinct features, the valence of Cu ions in $SrFe_{2-x}Cu_xAs_2$ single crystals is monovalent, regardless of the doping level.

The temperature dependences of the in-plane electrical resistivity for $SrFe_{2-x}Cu_xAs_2$ single crystals are shown in Fig. 3. In Fig. 3(a), the resistivity exhibits an obvious anomaly at a temperature from 196 K for $SrFe_2As_2$ to 71 K for the samples slightly doped with Cu, which is associated with the structural/SDW transition reported previously.[21] The temperature of the structural/SDW transition T_{SDW} decreases with increasing Cu doping, and disappears when $x > 0.25$. The anomaly due to the structural/SDW transition becomes more pronounced with doping, which is similar to that of Mn- or Cr-doped $BaFe_2As_2$,[8,14] and in strong contrast with Co- or Ni-doped $BaFe_2As_2$.[6] Figure 3(b) shows the temperature dependence of resistivity for samples with $0.37 \leqslant x \leqslant 1.2$. The value of resistivity decreases quickly with increasing Cu doping, and the behavior of resistivity evolves from

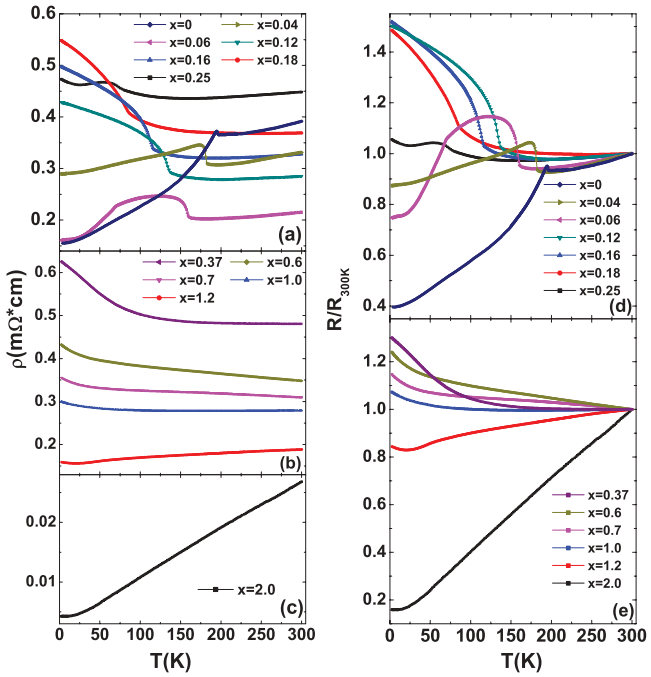

FIG. 3. (Color online) (a)–(c) Temperature dependence of in-plane electrical resistivity for $SrFe_{2-x}Cu_xAs_2$ single crystals. (d) and (e) Temperature dependence of the normalized resistivity to 300 K.

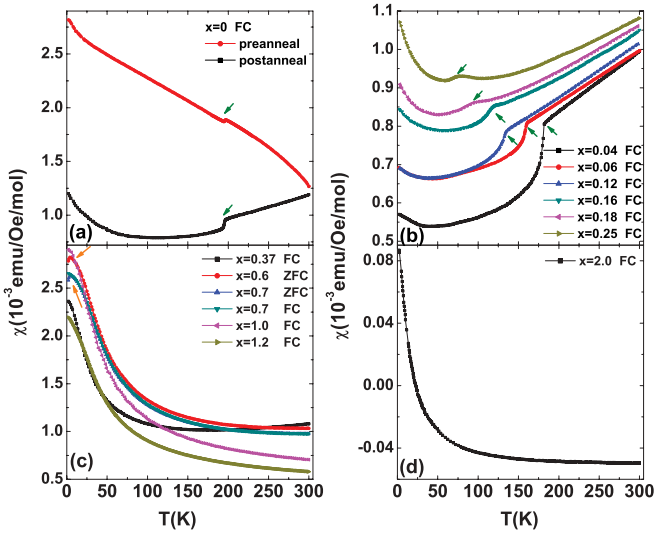

FIG. 4. (Color online) (a)–(d) Temperature dependence of magnetic susceptibility for $SrFe_{2-x}Cu_xAs_2$ ($0 \leqslant x \leqslant 2.0$) under a magnetic field of 5 T. The SDW transition temperature T_{SDW} is shown by green arrows. The orange arrow shows the spin-glass-like transition.

semiconducting to metalliclike. No anomaly is observed due to the structural or magnetic transition. For the samples with $x = 0.37$, 0.6, and 0.7, the temperature dependence of resistivity shows a semiconducting behavior through the entire temperature range, while for $x = 1.0$, the resistivity exhibits metallic behavior above 190 K, and then turns into a semiconducting behavior. For $x = 1.2$, the resistivity is 0.19 mΩ cm at 300 K, which is one order of magnitude larger than that of $SrCu_2As_2$. The resistivity decreases with cooling, reaches a minimum around 20 K, and then turns upward. The resistivity of $SrCu_2As_2$ as a function of temperature is presented in Fig. 3(c), which is similar to the results reported previously.[17] The temperature coefficient of $\rho(T)$ is positive, indicating a metallic character. The values of residual resistivity ρ_0 and the residual resistivity ratio (RRR) are 4.2 μΩ cm and 6.4, respectively, indicating the high quality of the $SrCu_2As_2$ single crystals. The clear evolution of the resistivity behavior and phase transition are shown in Figs. 3(d) and 3(e).

Figure 4 presents the zero-field-cooled (ZFC) or field-cooled (FC) magnetic susceptibility χ for all the single crystals as a function of temperature from 2 to 300 K in an applied magnetic field H of 5.0 T aligned in the ab plane. Figure 4(a) presents the typical behavior of one $SrFe_2As_2$ single crystal before and after annealing at 300 °C for 5 h. The temperature dependence of χ exhibits an unusual behavior for the as-grown $SrFe_2As_2$, and changes to a universal behavior after annealing, agreeing with the previous report.[22] These phenomena are supposed to be related to the presence of lattice distortion in $SrFe_2As_2$.[23] For samples with $0 \leqslant x \leqslant 0.25$, as shown in Figs. 4(a) and 4(b), a structural/SDW transition is obviously observed and marked by green arrows, corresponding to the anomaly observed in the resistivity shown in Figs. 3(a) and 3(d). The $\chi(T)$ of samples with $0.37 \leqslant x \leqslant 1.2$ shows paramagnetic behavior in the whole temperature range, and no obvious magnetic transition was observed down to 2 K. The magnitude of χ decreases with increasing Cu doping, as shown in Fig. 4(c). Below 20 K, a small separation between the FC and ZFC curves for the crystal with $x = 0.7$ is observed, indicating a glasslike behavior. The χ of $SrCu_2As_2$ in Fig. 4(d) has a negative sign above 20 K, which is a typical behavior for a nonmagnetic metal and is consistent with the previous report.[17]

Figure 5(a) shows the typical derivatives of $\chi(T)$ and $\rho(T)$ to figure out the transition temperature T_{SDW}. Only one obvious peak is observed in both derivative curves of $\chi(T)$ and $\rho(T)$, corresponding to the temperature of the phase transition. T_{SDW} determined from derivatives of $\chi(T)$ and $\rho(T)$ are highly consistent with each other, as shown in Fig. 5(b). With increasing Cu doping, T_{SDW} decreases quickly from 196 K for $x = 0$ to 71 K for $x = 0.25$, which is similar to that of $Ba(Fe_{1-x}Cu_x)_2As_2$,[18] except that no superconductivity was observed in $SrFe_{2-x}Cu_xAs_2$ for any doping content.

To further understand the conducting carriers in the Cu-doped $SrFe_2As_2$ samples, the Hall coefficient (R_H) measurements were performed on the single crystals, as shown in Fig. 6. In Figs. 6(a) and 6(b), a distinct structural/SDW transition can be observed for samples $0 \leqslant x \leqslant 0.18$, consistent with the resistivity and susceptibility. The Hall coefficient is negative, indicating that electron-type carriers dominate, and the absolute value decreases with Cu doping content. For $0.25 \leqslant x \leqslant 1.2$, the Hall coefficients R_H are also negative in the whole temperature range, indicating that the dominated carrier is electron type. The absolute values of the Hall coefficients for $x = 0.25$ and 0.37 are smaller than those of samples with a lower Cu doping content. They increase

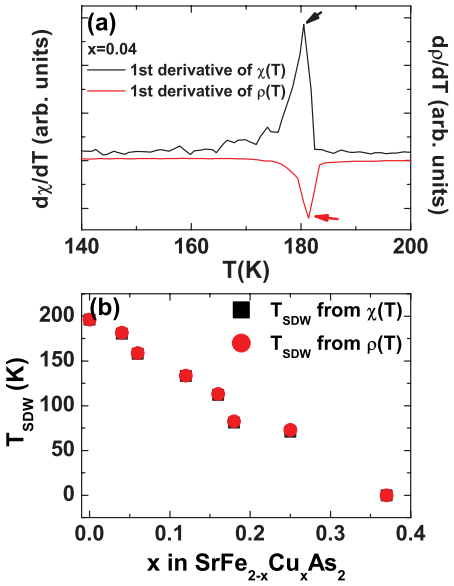

FIG. 5. (Color online) (a) The derivatives of $\chi(T)$ and $\rho(T)$ as a function of temperature for the $x = 0.04$ sample. The distinct peaks indexed by arrows in $d\chi(T)/dT$ and $d\rho(T)/dT$ curves are used to determine the temperature of the structural/SDW transition. (b) Evolution of T_{SDW} with Cu doping.

with cooling, reach maxima at around 40 K, and then slightly decline at low temperature. For $x = 0.25$, no phase transition is observed around the temperature corresponding to the structural/SDW transition, probably because its phase transition is too weak. A weak temperature dependence of the Hall coefficient is observed in the whole temperature region for samples with $x = 0.6$, 0.7 and 1.2. The absolute values of R_H for these three samples are very small with the same order of magnitude of 10^{-10} m^3/C, and decrease with further increasing Cu doping. As shown in Fig. 6(d), it is clear that the Hall coefficient of $SrCu_2As_2$ is positive in the whole temperature range, which suggests that the hole-type

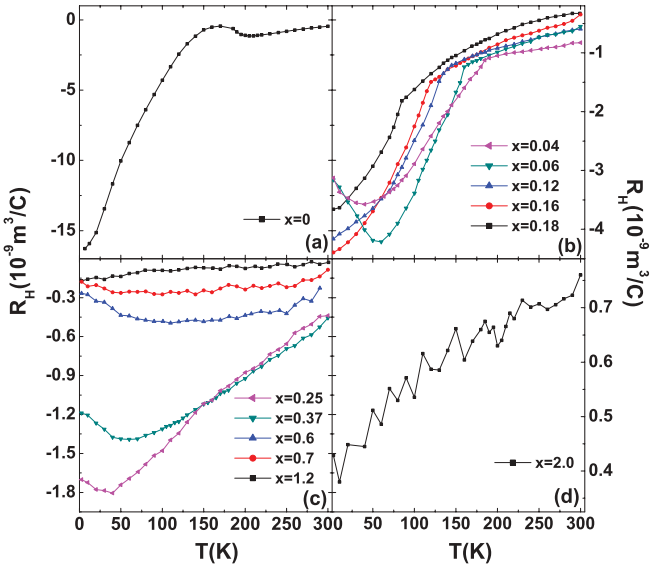

FIG. 6. (Color online) Temperature dependence of Hall coefficients R_H for $SrFe_{2-x}Cu_xAs_2$ samples.

carriers dominate. The value of R_H is 7×10^{-10} m^3/C at 300 K, which is remarkably small, indicating a relatively high density of charge carriers, estimated to be of the order of 10^{22} cm^{-3}. The magnitude and temperature dependence of the Hall coefficient for $SrCu_2As_2$ is similar to the reports.[24] In conclusion, with a gradual increase of Cu doping, the Hall coefficient changes from negative to positive, and its absolute value changes gradually. These results indicate that the carrier changes from electron type to hole type, and the concentration of the carrier changes simultaneously with Cu content. Combining with XPS results, it strongly suggests that partial Cu substitutions for Fe in $SrFe_2As_2$ may result in hole doping rather than the expected electron doping. This is probably the reason that Cu substitutions in iron-based materials cannot induce superconductivity.

To our knowledge, the valence state of Cu found in the previously reported pnictide oxides is always +1, because the anionic environment of the pnictide oxides is in general not sufficiently electronegative to oxidize Cu to +2. Even in the $LaNiO_2$-type $[M'O_2]$ layers of oxysulfides $Sr_2[M'_{1-x}Cu_x{}^{2+}O_2][Cu_2{}^{1+}S_2]$ (M' = Sc, Cr, Mn, Fe, Co, Ni, Zn), which are expected to have a more electronegative anionic environment than the pnictide oxides, the maximum Cu^{2+} content for the single-phase sample was $x < 1$.[25,26] This also indicates that the accommodation of Cu^{2+} in the weakly electronegative anionic environment of suboxides such as pnictide oxides and oxychalcogenides is difficult in contrast to its accommodation in the more electronegative anionic environment of the oxides.[27] Therefore, the valence state of Cu prefers +1 in the iron-based pnictide with a more weakly electronegative anionic environment, such as in $EuCuP$ (P = P, As, Sb),[28] BaCuAs, CaCuAs, $SrCu_2As_2$, $SrCu_2Sb_2$, and $BaCu_2Sb_2$.[17]

IV. CONCLUSION

In summary, XPS Cu $2p$ spectra, a deviation of V from Vegard's law, diamagnetic susceptibility, and a positive Hall coefficient indicate that the valence state of Cu in $SrCu_2As_2$ is +1 with a fully occupied $3d$ shell. The structural/SDW transition is suppressed with increasing Cu doping content for $x \leqslant 0.25$, and disappears when the Cu doping content x is higher than 0.25. Superconductivity cannot be induced over the whole doping range. The nearly same peak position of the Cu $2p$ core line as that in $SrCu_2As_2$ for all crystals and the evolution of Hall coefficients strongly suggest that partial Cu substitutions for Fe in $SrFe_2As_2$ may result in hole doping rather than the expected electron doping, which is the possible reason that Cu doping cannot induce superconductivity in $SrFe_{2-x}Cu_xAs_2$.

ACKNOWLEDGMENTS

This work is supported by the National Natural Science Foundation of China (Grants No. 11190021, No. 11174266, and No. 51021091), the "Strategic Priority Research Program (B)" of the Chinese Academy of Sciences (Grant No. XDB04040100), the National Basic Research Program of China (973 Program, Grants No. 2012CB922002 and No. 2011CBA00101), and the Chinese Academy of Sciences.

*Corresponding author: chenxh@ustc.edu.cn

[1]T. Yamazaki, N. Takeshita, R. Kobayashi, H. Fukazawa, Y. Kohori, K. Kihou, C. H. Lee, H. Kito, A. Iyo, and H. Eisaki, Phys. Rev. B **81**, 224511 (2010).

[2]F. Ishikawa, N. Eguchi, M. Kodama, K. Fujimaki, M. Einaga, A. Ohmura, A. Nakayama, A. Mitsuda, and Y. Yamada, Phys. Rev. B **79**, 172506 (2009).

[3]E. Colombier, S. L. Budko, N. Ni, and P. C. Canfield, Phys. Rev. B **79**, 224518 (2009).

[4]H. Chen, Y. Ren, Y. Qiu, Wei Bao, R. H. Liu, G. Wu, T. Wu, Y. L. Xie, X. F. Wang, Q. Huang, and X. H. Chen, Europhys. Lett. **85**, 17006 (2009).

[5]D. C. Johnston, Adv. Phys. **59**, 803 (2010).

[6]P. C. Canfield and S. L. Budko, Annu. Rev. Condens. Matter Phys. **1**, 27 (2010).

[7]S. Jiang, H. Xing, G. Xuan, C. Z. Ren, C. Feng, J. Dai, Z. Xu, and G. Cao, J. Phys.: Condens. Matter **21**, 382203 (2009).

[8]A. S. Sefat, R. Jin, M. A. McGuire, B. C. Sales, D. J. Singh, and D. Mandrus, Phys. Rev. Lett. **101**, 117004 (2008).

[9]C. Wang, Y. K. Li, Z. W. Zhu, S. Jiang, X. Lin, Y. K. Luo, S. Chi, L. J. Li, Z. Ren, M. He, H. Chen, Y. T. Wang, Q. Tao, G. H. Cao, and Z. A. Xu, Phys. Rev. B **79**, 054521 (2009).

[10]X. F. Wang, T. Wu, G. Wu, R. H. Liu, H. Chen, Y. L. Xie, and X. H. Chen, New J. Phys. **11**, 045003 (2009).

[11]L. J. Li, Q. B. Wang, Y. K. Luo, H. Chen, Q. Tao, Y. K. Li, X. Lin, M. He, Z. W. Zhu, G. H. Cao, and Z. A. Xu, New J. Phys. **11**, 025008 (2009).

[12]D. Kasinathan, A. Ormeci, K. Koch, U. Burkhardt, W. Schnelle, A. Leithe-Jasper, and H. Rosner, New J. Phys. **11**, 025023 (2009).

[13]Y. Liu, D. L. Sun, J. T. Park, and C. T. Lin, Physica C **470**, S513 (2010).

[14]J. S. Kim, S. Khim, H. J. Kim, M. J. Eom, J. M. Law, R. K. Kremer, J. H. Shim, and K. H. Kim, Phys. Rev. B **82**, 024510 (2010).

[15]A. S. Sefat, D. J. Singh, L. H. VanBebber, Y. Mozharivskyj, M. A. McGuire, R. Jin, B. C. Sales, V. Keppens, and D. Mandrus, Phys. Rev. B **79**, 224524 (2009).

[16]K. Marty, A. D. Christianson, C. H. Wang, M. Matsuda, H. Cao, L. H. VanBebber, J. L. Zarestky, D. J. Singh, A. S. Sefat, and M. D. Lumsden, Phys. Rev. B **83**, 060509(R) (2011).

[17]V. K. Anand, P. Kanchana Perera, Abhishek Pandey, R. J. Goetsch, A. Kreyssig, and D. C. Johnston, Phys. Rev. B **85**, 214523 (2012).

[18]N. Ni, A. Thaler, J. Q. Yan, A. Kracher, E. Colombier, S. L. Bud'ko, P. C. Canfield, and S. T. Hannahs, Phys. Rev. B **82**, 024519 (2010).

[19]D. J. Singh, Phys. Rev. B **79**, 153102 (2009).

[20]P. Steiner, V. Kinsinger, I. Sander, B. Siegwart, S. Hüfner, C. Politis, R. Hoppe, and H. P. Müller, Z. Phys. B **67**, 497 (1987).

[21]A. Jesche, N. Caroca-Canales, H. Rosner, H. Borrmann, A. Ormeci, D. Kasinathan, H. H. Klauss, H. Luetkens, R. Khasanov, A. Amato, A. Hoser, K. Kaneko, C. Krellner, and C. Geibel, Phys. Rev. B **78**, 180504(R) (2008).

[22]J.-Q. Yan, A. Kreyssig, S. Nandi, N. Ni, S. L. Budko, A. Kracher, R. J. McQueeney, R. W. McCallum, T. A. Lograsso, A. I. Goldman, and P. C. Canfield, Phys. Rev. B **78**, 024516 (2008).

[23]S. R. Saha, N. P. Butch, K. Kirshenbaum, J. Paglione, and P. Y. Zavalij, Phys. Rev. Lett. **103**, 037005 (2009).

[24]M. Qin, C. Yang, Y. Wang, Z. Yang, P. Chen, and F. Huang, J. Solid State Chem. **187**, 323 (2012).

[25]S. Okada, M. Matoba, S. Fukumoto, S. Soyano, Y. Kamihara, T. Takeuchi, H. Yoshida, K. Ohoyama, and Y. Yamaguchi, J. Appl. Phys. **91**, 8861 (2002).

[26]H. Hirose, K. Ueda, H. Kawazoe, and H. Hosono, Chem. Mater. **14**, 1037 (2002).

[27]T. C. Ozawa and S. M. Kauzlarich, Sci. Technol. Adv. Mater. **9**, 033003 (2008).

[28]G. Michels, S. Junk. W. Schlabitz, E. Holland-Moritz, M. M. AbdElmeguidt, J. Dünner, and A. Mewis, J. Phys.: Condens. Matter **6**, 1769 (1994).